Distorted body image in complex regional pain syndrome

G. Lorimer Moseley, PhD

Regional anesthesia results in shrinkage of the primary sensory cortex (S1) representation of the area and the perception that the area is larger than it is.[1] Complex regional pain syndrome type 1 (CRPS1) also involves shrinkage of S1 representation[2] and, anecdotally, the perception of marked swelling when none is apparent. We posited that if a reduced S1 representation of the affected limb is involved in generating a perception that the limb is larger than it really is, then this effect should be present in patients with CRPS1.

Methods. Fifty patients diagnosed with CRPS1[3] initiated by wrist or hand fracture and 18 patients with non-CRPS1 hand or wrist pain were eligible (see table E-1 on the *Neurology* Web site at www.neurology.org). Exclusion criteria were pain elsewhere (five patients with CRPS1), symptoms extending beyond the affected limb (four patients), psychiatric diagnosis (two patients), and unable to understand English (one patient). A 3,000-DPI, 4.8 × 3.2-cm digital photograph was taken of the two hands and distal one-third of the forearms, placed side by side. The image of the affected limb was compressed or expanded in one dimension to 85%, 90%, 95%, 100%, 105%, 110%, or 115% such that an expanded image made the limb look thicker but not longer than it was. Seven 4.2 × 2.8-cm images of the limb pairs (each incorporating one of the thickness manipulations of the affected hand) were positioned randomly on a 19-inch 1,280 × 1,024 resolution color monitor. Patients selected the photograph they believed to be accurate. Pilot data showed that image pair selection is reliable in patients with non-CRPS1 pain (intercorrelation coefficient [ICC] >0.93). The size of the affected limb was estimated by the ratio between limbs of the mean circumference taken midway along the proximal phalanx of fingers 2 to 4, using hand measuring tape (Beiersdorf-Jobst, Hamburg, Germany). This measure is reproducible (ICC >0.9). A Mann-Whitney *U* test was used to test the difference between the perceived sizes of the affected limb selected by subjects and controls. To identify whether the selected image was related to patient characteristics, linear regression between the selected image and finger circumference ratio, mean pain intensity, age of the patient, and duration of symptoms, with correction for multiple measures, was used. Assessors were blinded to the purpose of the study. Logistic regressions were run testing the relationship of the perceived relative size of the affected limb to the presence or absence of each medication, the presence of apparent swelling (to the investigator), and apparent atrophy (to the investigator). Patients gave informed consent. Procedures were approved by the institutional ethics committee and conformed to the Declaration of Helsinki.

Results. For patients with CRPS1, the median selection showed that the affected limb expanded to 105% of the actual width. The mean (SD) size of the affected limb in the selected image was 107% (3%). Sixty-three percent of patients with CRPS1 and 17% of the control group selected an image that showed the affected limb expanded (figure E-1). The selected image did not relate to finger circumference, pain intensity, or age ($p > 0.3$ for all) but did relate to duration of symptoms ($r = 0.55$, $F(1,36) = 15.5$, $p < 0.001$). There was no effect of medication, apparent swelling, atrophy, or side of affected limb between patients who selected enlarged images and those who did not ($p > 0.41$). In control patients, the median selection showed the affected limb at 100% and the mean (SD) width of the limb in the selected image was 100% (2%), which was smaller than that for patients with CRPS1 (Mann-Whitney $U = 136$, $Z = -3.7$, $p < 0.001$).

Discussion. Patients with CRPS1 perceived the affected limb to be larger than it really was. This distortion of body image may be an important part of the presentation of CRPS1. The mechanisms involved are not clear, but S1 changes may be involved. S1 changes have been proposed to underpin clinical phenomena (e.g., stimulation at one site referring sensation to body parts represented immediately adjacent to the affected area in S1[4]) that occur in patients following amputation, tooth extraction, spinal cord injury, stroke, local anesthesia, and CRPS1. Those groups also describe distortion of body image such that the anesthetized part feels large, full, or swollen. Perhaps through neural connections indirectly linking S1 and association cortices in the "what" visual pathway, shrinkage of the S1 representation of the affected limb engenders alteration of visual magnitude perception. It is notable that the perceived size of the affected limb related to the duration of CRPS1, and in other patient groups characterized by changes in S1 representation, e.g., amputees, cortical reorganization correlates with the duration of symptoms.[5]

The current sample was not homogeneous; symptoms, anatomic site, and medications varied. Although these factors did not relate to selected image, future work could elucidate the importance of such factors and verify the current results. The results corroborate other findings of distorted body image in people with CRPS1, but the mechanisms remain poorly understood.

Additional material related to this article can be found on the *Neurology* Web site. Go to www.neurology.org and scroll down the Table of Contents for the September 13 issue to find the link for this article.

From the School of Physiotherapy, The University of Sydney, Sydney, Australia.

Disclosure: G. Lorimer Moseley is supported by the National Health and Medical Research Council of Australia.

Received November 15, 2004. Accepted in final form April 21, 2005.

Address correspondence and reprint requests to Dr. G. Lorimer Moseley, Department of Human Anatomy & Genetics, University of Oxford, South Parks Road, Oxford OX1 3QX, United Kingdom; e-mail: lorimer.moseley@anat.ox.ac.uk

References

1. Gandevia S, Phegan C. Perceptual distortions of the human body image produced by local anaesthesia, pain and cutaneous stimulation. J Physiol (Lond) 1999;514:609–616.
2. Maihofner C, Handwerker HO, Neundorfer B, Birklein F. Patterns of cortical reorganization in complex regional pain syndrome. Neurology 2003;61:1707–1715.
3. Bruehl S, Harden RN, Galer BS et al. External validation of IASP diagnostic criteria for complex regional pain syndrome and proposed research diagnostic criteria. Pain 1999; 81: 147–154.
4. McCabe CS, Haigh RC, Halligan PW, Blake DR. Referred sensations in patients with complex regional pain syndrome type 1. Rheumatology 2003;42:1067–1073.
5. Flor H, Elbert T, Knecht S et al. Phantom-limb pain as a perceptual correlate of cortical reorganization following arm amputation. Nature 1995;375:482–484.

Editorial, see page 666
See also pages 748 and 751

CME VIDEO Ventilator self-cycling may falsely suggest patient effort during brain death determination

Eelco F.M. Wijdicks, MD; Edward M. Manno, MD; and Steven R. Holets, RTT

Brain death is suspected when a patient with a destructive neurologic brain injury on a ventilator fails to generate respirations and other brainstem reflexes are absent. An apnea test is mandated in brain-death evaluation. Apnea is concluded when no breathing effort is observed at $PaCO_2$ of 60 mm Hg or with a 20 mm Hg increase from normal baseline.[1] There are no reported cases of adult patients who were declared brain dead and later initiated respirations. Two cases from the U.K. (brain death and cardiac death) have been described where the ventilator readings were erroneous but remotely suggested patient effort.[2,3] We have recently come across several instances during brain-death determination when it appeared that patients falsely triggered the ventilator. We would like to call attention to this phenomenon of ventilator self-cycling.

Methods. From January 2002 to February 2005, we performed apnea tests in 83 patients in our neurologic-neurosurgical intensive care unit for brain-death determination. All patients fulfilled the clinical criteria of brain death and apnea tests were performed using the American Academy of Neurology Practice Parameter guidelines.[1] In four patients (aneurysmal subarachnoid hemorrhage in three patients and traumatic brain injury in one patient), we noted occasional "triggering" of the ventilator. The apnea test proved positive and remained positive after repeating the test (no breathing of patient after disconnection of the ventilator at $PaCO_2$ of 60 mm Hg or more). This false triggering of the ventilator disappeared after the flow-by trigger mechanism (typically set at –2 cm H_2O) was changed to pressure trigger mechanism (typically set at 2.0 L/min) or when the trigger sensitivity was adjusted upward. In one patient on an intermittent mandatory ventilation (IMV) of 10 and peak end-respiratory pressure (PEEP) of 5 cm of water, the displayed frequency correlated linearly with the sensitivity (sensitivity of 3.0 L/min; frequency of 10 breaths/min, sensitivity of 2.0 L/min; frequency of 13 breaths/min, sensitivity of 1.5 L/min; frequency of 15 breaths/min; sensitivity of 0.2 L/min, frequency of 19 breaths/min). To confirm the highly sensitive trigger mechanism of current mechanical ventilators, we conducted a brief experiment. An ICU ventilator PB 840 (Puritan Bennett, Pleasanton, CA) connected to a test lung (Michigan Instruments, Grand Rapids, MI) was used for this simulation. Ventilator settings were assist-control mode: respiratory rate, 12 breaths/min; tidal volume, 500 mL; inspiratory flow rate, 30 L/min; positive end expiratory pressure of 5 cm/H_2O; and maximum trigger sensitivity threshold, 0.2 L/min. Test lung settings used a Rp20 resistor, which is equivalent to a 6.5 endotracheal tube with a compliance of 0.05 L/cm H_2O (50 mL/cm H_2O).

Additional material related to this article can be found on the *Neurology* Web site. Go to www.neurology.org and scroll down the Table of Contents for the September 13 issue to find the link for this article.

Apnea simulation was conducted by switching the ventilator to a spontaneous mode of respiration with a pressure support of 0 cm H_2O and a PEEP of 5 cm H_2O (CPAP 5 cm H_2O). Upon completion of this change, the ventilator began to self-cycle with a frequency of 28 breaths/min with a tidal volumes of 90 mL (see video clip). Self-cycling was eliminated by increasing the trigger flow sensitivity threshold to 2.0 L/min.

Discussion. This simulation and patient examples demonstrate that ventilator settings below a certain trigger sensitivity threshold may cause the ventilator to self-cycle, simulating spontaneous respirations. Ventilator self-cycling may become apparent in clinical settings when factors other than the patient's inspiratory effort cause the trigger threshold value to be achieved. Common causes of ventilator self-cycling include leaks which could cause pressure changes, e.g., chest tube in polytraumatized patients; secretions or water in the ventilator circuit; or the cardiac cycle itself, which could change transpleural pressure and flow in a compliant lung. This phenomenon may be more common in new-generation ventilators that incorporate extremely sensitive flow trigger settings.[2-6] Ventilator self-cycling is a well-known phenomenon in the anesthesiology literature, although we believe it is not familiar to most neurologists involved in the declaration of brain death. If not recognized, it may suggest that patients with a major destructive brain injury can still "trigger the ventilator" even though all brainstem reflexes have disappeared. This may be interpreted as presence of respiratory function and could unnecessarily prolong the determination of brain death. In other instances, when the apnea tests result conflicts with the ventilator display of a possible spontaneous respiratory effort, it may lead to unnecessary confirmatory tests. We noted false triggering in 5% of apnea tests, but prospective studies could provide a more accurate prevalence and we suspect it is more common.

From the Division of Critical Care Neurology (Drs. Wijdicks and Manno) and the Department of Respiratory Care (S.R. Holets), Mayo Clinic College of Medicine, Rochester, MN.

The authors report no conflicts of interest.

Received March 3, 2005. Accepted in final form May 25, 2005.

Address correspondence and reprint requests to Dr. Eelco F.M. Wijdicks, Mayo Clinic College of Medicine Department of Neurology, W8B 200 First St. SW, Rochester, MN 55905; e-mail: wijde@mayo.edu

References

1. Wijdicks EFM. Determining brain death in adults. Neurology 1995;45:1003–1011.
2. Willatts SM, Drummond G. Brainstem death and ventilator trigger settings. Anaesthesia 2000;55:676–7.
3. Kannan S, Sinclair S. Spurious ventilator triggering in a dead patient. Anaesthesia 2002;57:710–731.
4. Schwab RJ, Schnader JS. Ventilator autocycling due to an endotracheal tube cuff leak. Chest 1991;100:1172–1173.
5. Imanaka H, Nishimura M, Takeuchiet al. Autotriggering caused by cardiogenic oscillation during mechanical ventilation. Crit Care Med 2000;28:402–407.
6. Mehta S, McCool FD, Hill NS. Leak compensation in positive pressure ventilators: a lung model study. Eur Respir J 2001;17:259–267.

Sympathetic activation due to deep brain stimulation in the region of the STN

A. Lipp, MD; J. Tank, MD; T. Trottenberg, MD; A. Kupsch, MD; G. Arnold, MD; and J. Jordan, MD

The autonomic nervous system is important in cardiovascular regulation. The peripheral autonomic nervous system is at least in part accessible to direct measurements. However, it is difficult to assess central autonomic nervous system function in humans and the role of CNS pathways in human autonomic regulation is poorly understood. In recent years, deep brain stimulation (DBS) of the basal ganglia has been used to alleviate motor symptoms in advanced Parkinson disease (PD) and other movement disorders. Although the impact of DBS on motor function is well described, little is known about DBS effects on nonmotor structures within the central components of the autonomic nervous system. Furthermore, DBS provides a unique opportunity to map autonomic pathways close to the stimulation site.

Additional material related to this article can be found on the *Neurology* Web site. Go to www.neurology.org and scroll down the Table of Contents for the September 13 issue to find the link for this article.

We studied five patients (three men, two women, aged 61 ± 7 years; see table E-1 on the *Neurology* Web site at www.neurology.org) treated bilaterally with a subthalamic nucleus (STN) stimulator for an advanced Parkinson syndrome. The deep brain stimulator leads were equipped with four separated electrodes (1.5-mm wide, 0.5-mm space in between). We continuously measured heart rate (electrocardiogram), respiration (thoracic bioimpedance) and blood pressure (radial artery indwelling catheter). Prior to the study, associated dysautonomia was ruled out in all individuals by

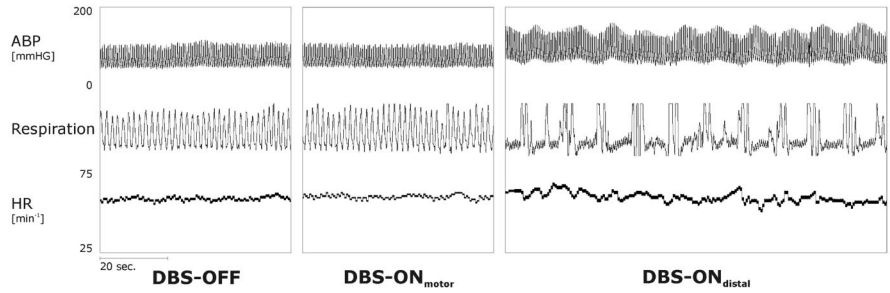

Figure. Arterial blood pressure (ABP), heart rate (HR), and respiration in a subthalamic nucleus–stimulated patient with Parkinson disease. All measurements remained unchanged when the proximal electrode was stimulated with 100 Hz (middle panel, ON_{motor}). When the distal electrodes were stimulated with 200 Hz, we observed rhythmic oscillations in blood pressure, heart rate, and respiration (right panel, ON_{distal}). DBS = deep brain stimulation.

a series of autonomic tests including valsalva maneuver as well as heart rate and blood pressure response to deep breathing and tilt test. All studies were approved by the local ethics committee and written informed consent was obtained before study entry.

After instrumentation, patients remained in a supine position and the DBS devices were adjusted for best motor control before recording the baseline. Then, the stimulator was switched off and the patients rested for at least 30 minutes before a second baseline was obtained. Finally, we tested the effect of different stimulation sites (proximal vs distal electrode) and the effect of different stimulation frequencies (10 Hz vs 200 Hz) on cardiovascular regulation. We correlated the physiologic response with the approximate electrode position in each patient using pre- and postoperative MRI.

Deep brain stimulation at the site of optimal motor response had no significant sustained effect on blood pressure, heart rate, or respiration in any patient. In comparison to previous reports,[1,2] none of the patients experienced any autonomic symptoms. Stimulation at the proximal electrode with either 200 Hz or 10 Hz had no major effects on autonomic parameters. However, in one patient, we observed profound autonomic responses that were related to both the stimulation site and stimulation frequency. In this patient, distal high frequency stimulation elicited immediate and profound sweating in face, neck, and upper part of the chest. After a 5-minute stimulation period, the patient began to shiver. The symptoms were associated with 0.05 Hz sinusoidal oscillations in blood pressure and in respiration (figure) and an elevation of mean arterial pressure (baseline: 82 mm Hg; stimulation: 103 mm Hg). These responses were rapidly reversible when the stimulator was switched back to the setting for the best motor control. We reproduced symptoms and associated physiologic changes on three occasions on two separate days. During the testing, the patient never reported other side effects such as dysarthria, visual disturbances, or painful tingling.

The postoperative MRI confirmed a correct position of the stimulation electrodes within the STN in four patients; none of them reported autonomic symptoms. In the patient with an autonomic response, the right and, to a lesser degree, the left electrode projected to a position posteromedial of the subthalamic nucleus. In this patient, superimposition of the MRI onto an anatomic plate[3] shows that the distal contacts of both stimulators extend to the posteromedial hypothalamus (triangle of Sano) and the lateral hypothalamic area (figure E-1).

We observed marked and reproducible changes in blood pressure regulation, sweating, and breathing pattern in a deep-brain–stimulated patient with an electrode located outside the subthalamic nucleus. The pressor response and the increased sweating are consistent with sympathetic activation. Chemical activation of the lateral hypothalamic area decreases blood pressure and heart rate,[4] whereas lesions of the posterior hypothalamus result in disturbances of the sweating mechanism.[5] Studies in rats have implicated dorsomedial hypothalamic sites in tachycardic responses, thermogenesis, and stress responses.[6] Although the exact mechanism by which electrical stimulation modulates neural function is unknown, higher frequency stimulation apparently elicits a depolarization block of adjacent neurons.[7] In our patient, electrical inhibition of an inhibitory autonomic pathway may have disclosed a central sympathetic rhythm. However, the observed phenomenon may also result from a stimulation of passing fibers.

Our study suggests that the lateral hypothalamic area and the posteromedial hypothalamus are important in human sympathetic regulation. Systematic physiologic studies in patients with brain stimulators may help to identify and to validate central autonomic pathways. The clinical implication of our observation is that patients with stimulator electrodes in atypical posteromedian positions should be carefully monitored for autonomic side effects.

From the Department of Neurology (Drs. Lipp, Trottenberg, Kupsch, and Arnold) and the Franz-Volhard Clinical Research Center (Drs. Tank and Jordan), Medical Faculty of the Charité, Berlin, Germany.

The authors report no conflicts of interest.

Received December 4, 2004. Accepted in final form May 25, 2005.

Address correspondence and reprint requests to Dr. Axel Lipp, Neurologische Poliklinik, Charité-Campus Virchow Klinikum, Augustenburger Platz 1, 13353 Berlin, Germany; e-mail: axel.lipp@charite.de

References

1. Kaufmann H, Bhattacharya KF, Voustianiouk A, Gracies JM. Stimulation of the subthalamic nucleus increases heart rate in patients with Parkinson disease. Neurology 2002;59:1657–1658.
2. Thornton JM, Aziz T, Schlugman D, Paterson DJ. Electrical stimulation of the midbrain increases heart rate and arterial blood pressure in awake humans. J Physiol 2002;539:615–621.
3. Schaltenbrand G, Wahren W. Atlas for stereotaxy of the human brain. Stuttgart: Georg Thieme Verlag, 2004.
4. Benarroch E. Functional anatomy of the CAN, In: Benarroch E, ed. Central autonomic network: Functional organization and clinical correlations, 1st ed. Armonk: Futura Publishing Company, 1997:29-60.
5. Smith CD. A hypothalamic stroke producing recurrent hemihyperhidrosis. Neurology 2001;56:1394–1396.
6. DiMicco JA, Samuels BC, Zaretskaia MV, Zaretsky DV. The dorsomedial hypothalamus and the response to stress: part renaissance, part revolution. Pharmacol Biochem Behav 2002;71:469–480.
7. Volkmann J. Deep brain stimulation for the treatment of Parkinson's disease. J Clin Neurophysiol 2004;21:6–17.

Motor-sensory neuropathy with minifascicle formation in a woman with normal karyotype

A. Malandrini, MD; S. Gambelli, MD; M. Muglia, PhD; G. Berti, BSc; A. Patitucci, PhD; K. Sugie, MD, PhD; F. Umehara, MD, PhD; A. Quattrone, MD; M.T. Dotti, MD; and A. Federico, MD

Minifascicle neuropathy (MN) is a rare developmental malformation of the peripheral nerve characterized by many small fascicles.[1] Two unrelated cases, in which the disorder was associated with 46XY pure gonadal dysgenesis (GD),[1,2] have been reported.

We report a 28-year-old woman with healthy unrelated parents. Two siblings of the father had walking difficulties, but they were not available for examination. Developmental milestones were normal. From age of 2 to 3 years, walking difficulty was noted. At 3 years, the patient was hospitalized and "hypotonic syndrome" was diagnosed. Symptoms were slowly progressive. At 28 years, neurologic examination suggested hereditary motor-sensory polyneuropathy (HMSN): difficulty in walking with bilateral stepping; weakness and hypotrophy of the distal muscles of the four limbs, especially tibialis anterior; reduced superficial sensation; more accentuated distally and absent deep tendon reflexes. EKG showed sinus bradycardia. Gynecological and pelvic ultrasound examinations were normal; sexual characteristics and 46XX caryotype were both normal. EMG showed neurogenic changes with denervation at rest (positive sharp waves and fibrillations) in both tibialis anterior muscles and fasciculation in the first dorsal interosseous. There was moderately reduced motor unit recruitment in tibialis anterior, first dorsal interosseous, biceps brachii, and quadriceps muscles. Sensory action potentials of the right median nerve were absent after stimulation of third finger, recording at the wrist, and stimulation of the sural nerves, recording at the ankle. There was reduced conduction velocity of the right median nerve (38.0 m/s; ampitude 2 mV) and right deep peroneus (33.2 m/s; amplitude 1.5 mV) recording at the tibialis anterior muscle. Compound muscle action potential of the deep peroneus, recorded at the brief extensor digitorum brevis, could not be elicited. The overall findings suggested severe axonal sensory-motor neuropathy.

Nerve biopsy study. Semithin sections showed that the nerve was made up of 26 small fascicles (figure 1A; normal values [NV] of 10 normal adult sural nerves: 4 to 8), ranging in diameter from 29 to 179 μm. The area of the single fascicles ranged between 880 and 38,000 μm^2 (NV: 45,000 to 225,000 μm^2), with a mean area of nerve of 15,895 μm^2 (NV: 90,320 ± 17,790 μm^2). The density of myelinated fibers in fascicles larger than 40 μm was greatly reduced (3,987/mm^2; NV: 8,000 to 12,000/mm^2); large diameter fibers were almost absent. The smallest fascicles contained only a few myelinated fibers. Many fibers had a relatively thin myelin sheath and several atypical onion bulb formations were observed. Perineurial cell processes tended to invade the endoneurium and split the fascicles (figure 1B). Occasional axonal degeneration was evident. Fiber teasing showed 5% of degenerating fibers with myelin ovoids, 4% with signs of deremyelination, and 6% fibers with short internodes. Ultrastructural examination showed that the perineurium consisted of few cell layers, even in large fascicles.

Molecular analysis. No mutation was found in the three exons of the *DHH* gene or in the sex-determining region Y (*SRY*) gene. No mutations were detected in *PMP22*, *P0*, or *EGR2* genes.

Discussion. Minifascicle neuropathy may occur as focal lesion after traumas[1] and with particular histologic features in perineuriomas. In perineuriomas, the perineurial cells form whorls consisting of concentric layers of spindle cells encircling the nerve fibers, leading to microfasciculation. Fascicles of reduced size, but normal in number, have been described in hereditary sensory-autonomic neuropathies (HSANs).[2-5] However, MN is described as an entity in its own right, unrelated to the above causes, in two patients with motor-sensory polyneuropathy[1-3] and XY pure GD, in only one of whom a homozygous mutation in the *DHH* gene was found.[1,3] Neither patient had mutation in the *SRY* gene, which is often involved in GD. *DHH* has been demonstrated to play a role in male gonadal development and spermatogenesis in humans,[4] and mutations of the gene may be partly responsible for 46XY GD.[3] *DHH* is also implicated in development of the peripheral nerve sheath.[1,5] In *DHH* mice,[4,6] there is the extensive formation of multiple, small, irregular minifascicles in peripheral nerves.

In the present case, we failed to detect any mutations in *DHH*, *SRY*, *PMP22*, *P0*, or *EGR2* genes. As in the previously reported cases, our biopsy findings suggested axonal neuropathy; however, in the above cases, the fascicles were more numerous, smaller, and with more evident structural disorganization (microfasciculation). The most remarkable difference was that minifascicle neuropathy was not associated with XY GD in our case. We suggest that HMSN syndromes with MN may exist independently of XY GD, caused by unidentifield genes involved in perineurial differentiation.

From the Department of Neurological and Behavioural Sciences, University of Siena, Siena, Italy (Drs. Malandrini, Gambelli, Dotti, and Federico, G. Berti); Institute of Neurological Sciences, National Research Council, Piano Lago di Mangone, Cosenza, Italy (Drs. Muglia, Patitucci, and Quattrone); the Department of Neurology, Nara Medical University, Nara, Japan (Dr. Sugie); Institute of Neurology, University "Magna Grecia," Catanzaro, Italy (Dr. Quattrone); Third Department of Internal Medicine, Kagoshima University School of Medicine, Kagoshima, Japan (Dr. Umehara).

The authors report no conflicts of interest.

Received January 26, 2005. Accepted in final form May 23, 2005.

Address correspondence and reprint requests to Dr. Alessandro Malandrini, Department of Neurological and Behavioural Sciences, University of Siena, Viale Bracci, 53100 Siena, Italy; e-mail: malandrini@unisi.it

References

1. Umehara F, Yamaguchi N, Kodama D, et al. Polyneuropathy with minifascicle formation in a patient with 46XY mixed gonadal dysgenesis. Acta Neuropathol 1999;98:309–312.
2. Sugie K, Futamura N, Tate G, Umehara F. Hereditary motor and sensory neuropathy with minifascicle formation in a patient with 46XY pure gonadal dysgenesis: a new clinical entity. Ann Neurol 2002;51:385–388.
3. Umehara F, Tate G, Itoh K, et al. A novel mutation of *desert hedgehog* in a patient with 46XY partial gonadal dysgenesis accompained by minifascicular neuropathy. Am J Hum Genet 2000;67:1302–1305.
4. Mirsky R, Rjessen K. The neurobiology of Schwann cells. Brain Pathology 1999;9:293–311.
5. Parmantier E, Lynn B, Lawson D, et al. Schwann cell-derived Desert hedgehog controls the development of peripheral nerve sheaths. Neuron 1999;23:713–724.
6. Bitgood MJ, Shen L, McMahon AP. Sertoli cell signaling by Desert hedgehog regulates the male germline. Curr Biol 1996;6:298–304.

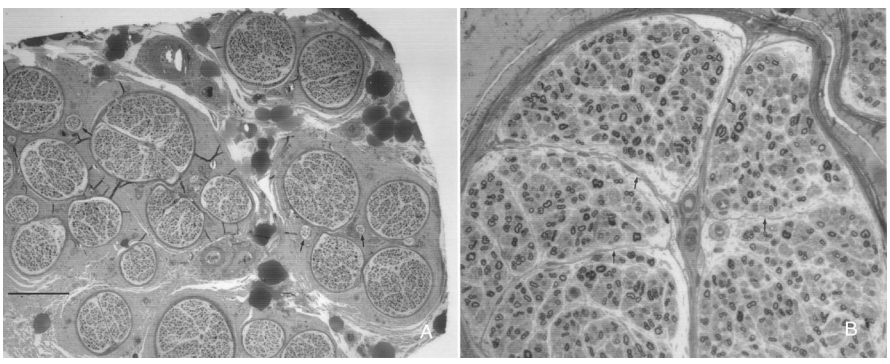

Figure. Sural nerve biopsy. Semithin section, toluidine blue. (A) The nerve consists of many small fascicles. Smaller fascicles (arrows) contain very few myelinated fibers. Bar = 100 μm. 50× magnification. (B) Some processes of perineurial cells extending into the endoneurium (arrows) and splitting fascicles. 300× magnification.

Resective surgery for epileptogenic dysembryoplastic neuroepithelial tumor in hemimegalencephaly

N. Specchio, MD; P. Kahane, MD; B. Pasquier, MD; L. Tassi, MD; and R. Guerrini, MD

Hemimegalencephaly (HME) is a severe and heterogeneous condition[1] with a wide spectrum of clinical and anatomic severity,[2] characterized by an enlarged and dysplastic hemisphere. MRI shows a simplified gyral pattern, with thickened gray matter, blurring of gray-white matter, and enlarged lateral ventricles.[3] Histologic abnormalities include giant neurons and balloon cells[3] resembling focal cortical dysplasia. Although focal cortical dysplasia and dysembryoplastic neuroepithelial tumors (DNT) share common histologic characteristics,[4] an association of DNT with an enlarged hemisphere has not been reported.

Treatment of medically resistant epilepsy associated with HME is based on functional hemispherectomy or disconnection of the malformed hemisphere (hemispherotomy).[5]

We present a patient who had a homogeneously enlarged hemisphere with a discrete structural abnormality in the temporal lobe. Intractable complex partial seizures were successfully treated with temporal resection and the resected tissue showed changes consistent with DNT.

Case report. This 25-year-old right-handed man had normal neurologic and cognitive development, along with bursts of aggressive behavior. From age 3 years, he had multiple per day episodes of unresponsiveness, staring, and pallor lasting several seconds, often followed by generalization. Antiepileptic drugs were ineffective. From age 8 years, he had an initial epigastric sensation, intense fear, and auditory symptoms. He would scream and run about asking for help and hugging bystanders; these symptoms were followed by staring and, often, left tonic-clonic manifestations. MRI showed an enlarged right hemisphere, with high-signal intensity limited to the temporal lobe (figure, A; see page 778). At age 10 years, he underwent partial resection of the right temporal lobe in another center (figure, B) without benefit. At age 14 years, we considered a second operation. Interictal EEG showed repetitive right temporal spikes, maximum over the T_6 electrode. Video-EEG–recorded seizures were accompanied by a right unilateral electrodecremental event. His verbal IQ (Wechsler Intelligence Scale for Children) was 92 and performance IQ was 65.

At age 15 years, he underwent removal of the right temporal pole, uncus, amygdala, and hippocampus (figure, C). During 9 year follow-up, no further seizures occurred and remarkable improvement in behavior was reported. Neuropathology (figure, D through K) revealed a lesion producing blurring between gray and white matter due to tumoral infiltration that was composed by a fibrillar structure with a mixture of glial small round or oval cells and ganglion cells, sometimes binucleated. There was plial thickening associated to disorganization of the cortical architecture with loss of lamination and binucleated neurons. In the surrounding tissue, there was plurinodular tumoral proliferation with cortical prevalence, characterized by alveolar appearance, a mixture of oligodendroglia-like cells, neurons floating within cystic spaces, and scattered astrocytes. The tumoral lesion was also present in the uncus and hippocampus. These histopathological changes were compatible with a complex form of DNT.[4]

Discussion. The clinical presentation of HME varies according to its anatomic severity,[1] ranging from rare individuals with normal cognitive level and no obvious dysplasia[5] to others with severe anatomoclinical impairment. Most cases are severe and have early-onset intractable multilobar seizures, which provide an indication for hemispherectomy or hemispherotomy.[6,7] In our patient, MRI, seizure semiology, and EEG findings prompted a right temporal resection, resulting in disappearance of the seizures and behavioral improvement.

In the most severe cases of HME, neuropathology shows widespread cytoarchitectural abnormalities, lack of alignment in the horizontal layers, and poor gray-white matter demarcation,[3] with giant neurons and "balloon cells."[3] However, in less severe cases, structural changes have regional predominance (so-called partial HME) and could be treated with multilobar resection if the epileptogenesis is also regional.[8]

In our patient, the epileptogenic tissue could be entirely removed. Histologic findings were compatible with DNT. Association of DNT with an enlarged hemisphere was previously unknown but it is not entirely surprising. Indeed, complex forms of DNT are characterized by foci of cortical dysplasia, which are combined with more characteristic changes including a specific glioneuronal element with columnar appearance, as well as glial nodules with an oligodendrocytic or astrocytic component.[4] Focal cortical dysplasia, in turn, bears close histologic similarities with HME, only differing in extent. Association between DNT and cortical dysplasia suggests that DNT may arise from a dysplastic focus or foci, although a neoplastic pathogenesis or a multifocal developmental abnormality remains the most likely basis of its origin.[4]

Each patient with HME must be individually assessed, as a standard approach could be misleading in a heterogeneous disorder. A limited resection may be an option in rare patients with discrete epileptogenesis.

From the Epilepsy, Neurophysiology and Neurogenetics Unit, Division of Child Neurology and Psychiatry, University of Pisa and Research Institute, IRCCS Stella Maris Foundation, Pisa, Italy (Drs. Specchio and Guerrini); the Department of Neuroscience and INSERIM 318 Research Unit, Grenoble Hospital, France (Dr. Kahane); the Department of Pathology, Section of Neuropathology, Centre Hospitalier Universitaire, Grenoble, France (Dr. Pasquier); and Epilepsy Surgery Center "C. Munari," Niguarda Hospital, Milan, Italy (Dr. Tassi).

Disclosure: The authors report no conflicts of interest.

Received March 9, 2005. Accepted in final form May 18, 2005.

Address correspondence and reprint requests to Dr. Renzo Guerrini, Epilepsy, Neurophysiology and Neurogenetics Unit, Division of Child Neurology and Psychiatry, University of Pisa and Research Institute IRCCS Stella Maris Foundation, Via dei Giacinti 2, 56018 Pisa, Italy; e-mail: renzo.guerrini@inpe.unipi.it

References

1. Guerrini R, Andermann E, Avoli M, Dobyns WB. Cortical dysplasias, genetics, and epileptogenesis. Adv Neurol 1999;79:95–121.
2. Robain O. Introduction to the pathology of cerebral cortical dysplasia. In: Guerrini, R, Andermann F, Canapicchi R, Rojer J, Zifkin BG, Pfanner P, eds. Dysplasias of cerebral cortex and epilepsy. New York: Lippincott-Raven, 1996:1-9.
3. Barkovich AJ, Kuzniecky RI, Jackson GD, Guerrini R, Dobyns WB. Classification system for malformations of cortical development: update 2001. Neurology 2001;57:2168–2178.
4. Dumas-Duport C. Dysembryoplastic neuroepithelial tumors. Brain Pathol 1993;3:283–295.
5. Fusco L, Ferracuti S, Fariello G, Manfredi M, Vigevano F. Hemimegalencephaly and normal intellectual development. J Neurol Neurosurg Psychiatry 1992;55:720–722.
6. Di Rocco C. Surgical treatment of Hemimegalencephaly. In: Guerrini, R, Andermann F, Canapicchi R, Rojer J, Zifkin BG, Pfanner P, eds. Dysplasias of cerebral cortex and epilepsy. New York: Lippincott-Raven, 1996: 295-304.
7. Villemure JG, Meagher-Villemure K, Montes JL, Farmer JP, Broggi G. Disconnective hemispherectomy for hemispheric dysplasia. Epileptic Disord 2003;5(S2):125–130.
8. D'Agostino, MD, Bastos A, Piras C, et al. Posterior quadrantic dysplasia or hemi-hemimegalencephaly: a characteristic brain malformation. Neurology 2004;62:2214–2220.

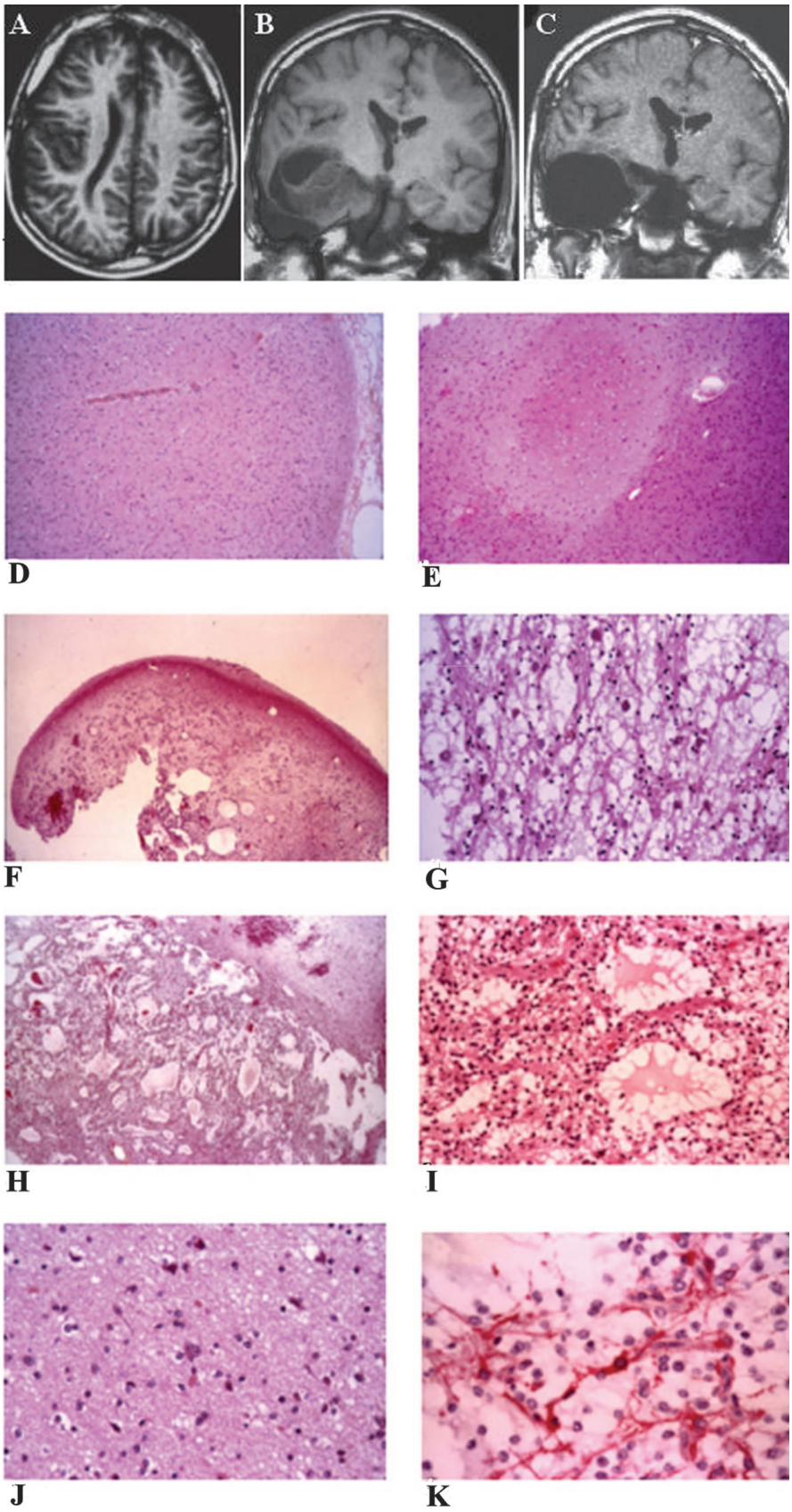

Figure 1. (A) Axial T1-weighted MRI shows right hemimegalencephaly. The right hemisphere is enlarged, with high signal in the temporal lobe. (B) Coronal T1-weighted image shows partial resection of the right temporal lobe, a heterogeneus signal increase in the white matter, and severe alteration of cortical architecture. (C) Coronal T1-weighted postsurgical image showing removal of right temporal pole, uncus, amygdale, and hippocampus. (D) Focus of dysplastic disorganization with loss of lamination in the temporal neocortex (HES 25×). (E) Microscopic focus of cortical nodular heterotopia in the white matter adjacent to the temporal horn of ventricle (HES 25×). (F) A poorly demarcated diffuse DNT in the anterior part of the hippocampus (HES 25×). (G) Specific glioneuronal element made of a mixture of oligodendroglia-like cells, scattered astrocytes, and neurons floating within cystic spaces (HES 250×). (H and I) Tumoral nodule composed predominantly of astrocytes and resembling pilocytic astrocytoma (H, HES 25×; I, HES 250×). (J) A binucleated neuron (center) at the periphery of a tumoral nodule (HES 250×). (K) Some astrocytes are immunoreactive for GFA protein (immunoperoxidase 400×).